



## Controlled peel testing of a model tissue for diseased aorta



Christopher Noble<sup>a,\*</sup>, Nicole Smulders<sup>b</sup>, Roger Lewis<sup>d</sup>, Matt J. Carré<sup>d</sup>, Steve E. Franklin<sup>b</sup>, Sheila MacNeil<sup>c</sup>, Zeike A. Taylor<sup>a</sup>

<sup>a</sup> CISTIB, Centre for Computational Imaging and Simulation Technologies in Biomedicine, INSIGNEO Institute for in silico Medicine, Department of Mechanical Engineering, The University of Sheffield, Sheffield, UK

<sup>b</sup> Philips Research, Eindhoven, The Netherlands

<sup>c</sup> Department of Materials Science and Engineering, The Kroto Research Institute, North Campus, University of Sheffield, Broad Lane, Sheffield, UK

<sup>d</sup> Department of Mechanical Engineering, The University of Sheffield, Sheffield, UK

### ARTICLE INFO

#### Article history:

Accepted 30 September 2016

#### Keywords:

Diseased tissue model  
Porcine aorta  
Collagenase  
Elastase  
Glutaraldehyde  
Dissection

### ABSTRACT

In this study, we examine the effect of collagenase, elastase and glutaraldehyde treatments on the response of porcine aorta to controlled peel testing. Specifically, the effects on the tissue's resistance to dissection, as quantified by critical energy release rate, are investigated. We further explore the utility of these treatments in creating model tissues whose properties emulate those of certain diseased tissues. Such model tissues would find application in, for example, development and physical testing of new endovascular devices. Controlled peel testing of fresh and treated aortic specimens was performed with a tensile testing apparatus. The resulting reaction force profiles and critical energy release rates were compared across sample classes. It was found that collagenase digestion significantly decreases resistance to peeling, elastase digestion has almost no effect, and glutaraldehyde significantly increases resistance. The implications of these findings for understanding mechanisms of disease-associated bio-mechanical changes, and for the creation of model tissues that emulate these changes are explored.

© 2016 The Authors. Published by Elsevier Ltd. This is an open access article under the CC BY license (<http://creativecommons.org/licenses/by/4.0/>).

### 1. Introduction

Arterial dissection refers to separation of the inner layers of the arterial wall. This is almost always initiated by trauma, either directly to the vessel wall, e.g. a catheter piercing or tearing the intimal layer of the vessel during an endovascular procedure (Mamas et al., 2008), or indirectly via external trauma, for instance from motor vehicle crashes (Srivastava et al., 2008). Depending on the direction of blood flow, the circulatory pressure will either press the tissue flap to the wall or act to propagate the dissection (Fig. 1). The former often results in the dissection remaining benign, whereas the latter can eventually progress to create a large tissue flap that blocks downstream blood flow in the true lumen and encourages flow into the newly formed false lumen between the flap and remaining artery wall. In large arteries this is often fatal: mortality rates for aortic dissections are reported to be 50% (Anagnostopoulos et al., 1972).

The increasing use of endovascular treatment methods renders desirable the development of new medical devices such as endovascular catheters. Research in this area requires access to large supplies of arterial tissue - preferably diseased, to reflect the state of real patient tissues - for physical testing of designs. But,

accessing human diseased tissue is costly and has numerous ethical and legal implications. Recently, we proposed porcine arterial tissue, processed with a suitable combination of enzyme solutions, as a model of diseased human tissues for use in such developments (Noble et al., 2016). Various enzymatic treatments were explored as a means of emulating the effects of diseases on the mechanical properties. Correspondingly, the effects of collagenase, elastase and glutaraldehyde treatments on the uniaxial elastic and failure behaviour of arterial tissues were investigated. In the present work, we expand on those results by investigating the effects of these treatments on dissection resistance. More specifically, we compare the mode 1 critical energy release rate ( $G_c$ ), as a measure of the strength of the tissues, before and after treatment with each of the mentioned solutions. The cheapness and ready availability of porcine arterial tissue (often considered a waste product in meat preparation), and avoidance of aforementioned ethical issues, suggests tissue models produced in this way can ameliorate the cost and complexity of medical device design.

The media of the arterial wall is most prone to dissection, as a result of its organisation into lamella units, stacked on top of one another (Wolinsky and Glagov, 1967). These lamellae are primarily composed of fibres of rubber-like elastin and stiffer collagen, and smooth muscle cells. These constituents, moreover, are oriented predominantly within planes tangential to the vessel axis, and with a bias towards circumferential directions over axial (Clark and Glagov,

\* Corresponding author.

E-mail address: [mta08cn@sheffield.ac.uk](mailto:mta08cn@sheffield.ac.uk) (C. Noble).

1985). This organisation in turn imparts the highest mechanical strength in circumferential directions, somewhat lower strength in axial directions, and significantly lower strength in radial directions (Schriebl et al., 2012; MacLean et al., 1999). This can be seen in Fig. 2.

Various diseases are associated with higher susceptibility to arterial dissection. For individuals with Marfan's syndrome the most common cardiovascular complication is enlargement of the ascending aorta, often leading to aortic dissection (Milewicz et al., 2005). This is caused by a mutation to the fibrillin-1 glycoprotein which in turn affects elastin protein structure in the thoracic aorta, resulting in a weakened arterial wall (Wityk et al., 2002). A further disease linked to increased dissection incidence is Ehlers-Danlos syndrome, which is associated with a mutation in the gene coding for collagen III. This again leads to

weakened arterial walls, with rupture or dissection the most common form of death (Ulbricht et al., 2004; Goldfinger et al., 2014). It was also speculated that low collagen content related to post-partum hormonal imbalance is associated with instances of arterial dissection (Bonnet et al., 1986). Additionally many cases of dissection accompany aneurysm formation and this is again linked to a change in the structure of both elastin and collagen (Adams et al., 1982; He and Roach, 1994; de Figueiredo Borges et al., 2008). Finally, there is also experimental evidence for diminution of vessel strength (specifically, aorta) associated with these diseases, which could explain this higher susceptibility (Sommer et al., 2016, 2008).

Enzyme digestion has been utilised previously to alter arterial mechanical properties. Treatment with collagenase or elastase was applied to reduce or remove the respective proteins, and the resulting changes in mechanical response were investigated via uniaxial, biaxial or inflation testing (Kochová et al., 2012; Weisbecker et al., 2013; Gundiah et al., 2013). However, little investigation of the effects on failure behaviour of the tissues, such as during dissection, has been performed. Those studies that have been performed were concerned with tensile failure modes (Dadgar et al., 1997; Noble et al., 2016). In contrast, characterisation of dissection properties in *untreated* tissue has been well investigated. Dissection propagation was first investigated by infusing liquid into the media to mimic the process of blood flow initiating and propagating a dissection (Hirst and Johns, 1962; Roach and Song, 1994; Carson and Roach, 1990). Later, Sommer et al. performed controlled peeling of the aortic media and recorded the force displacement behaviour (Sommer et al., 2008). This method has been used with tissue from complex sites like bifurcations (Tong et al., 2011), and with diseased human thoracic aortic and abdominal aortic aneurysms (Tong et al., 2014; Pasta et al., 2012).

Controlled peeling in this way clearly represents a simplification of *in vivo* loading regimes, and it could be argued that liquid infusion experiments more closely resemble blood flow-driven dissection, at least. In the latter configuration, while the separation of vessel layers would remain predominantly mode 1 (Fig. 3), there is likely an ambiguous mixture of rupture modes involved in any particular experiment. It is correspondingly difficult to extract meaningful and repeatable measures of tissue strength by this means. Peeling, by contrast, involves pure mode 1 rupture, and the physical meaning of the derived energy release rate  $G_c$  is correspondingly clear. The rupture process, being driven by displacements of opposing tissue flaps, is also easier to control, further improving repeatability. Therefore, as a means of quantifying resistance to dissection (i.e. separation of tissue layers), and of reliably assessing the effect on this of the different treatments, peeling tests were adopted in this work.

The remainder of the paper is structured as follows: in Section 2, the preparation of tissue samples, and the mechanical testing procedures are described; in Section 3, experimental results are summarised; and

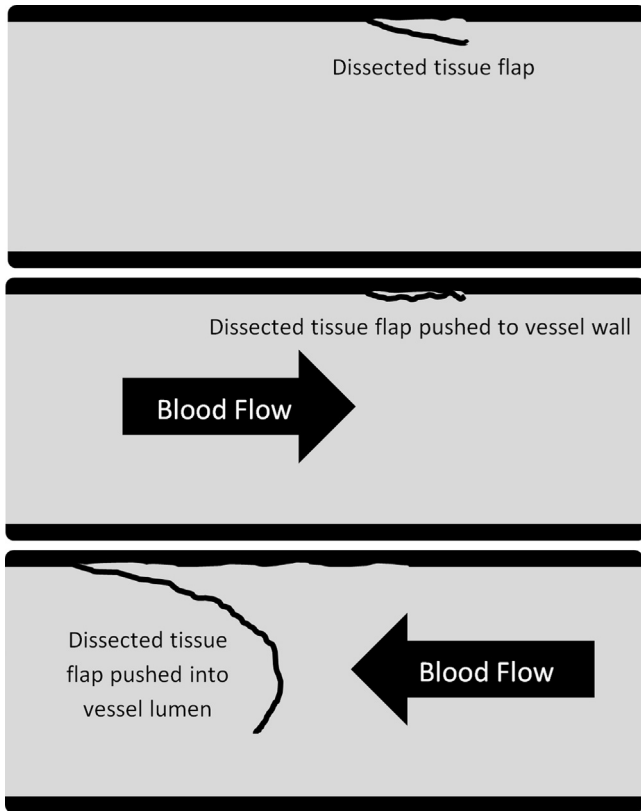


Fig. 1. Schematic detailing dissection becoming benign or propagating depending on blood flow direction. Top, initial dissection with tissue flap extending in to vessel lumen. Middle, tissue flap pushed back onto vessel wall by blood flow. Bottom, further tissue peeled from vessel wall by blood pressure, with the tissue flap now obscuring a large portion of the vessel lumen.

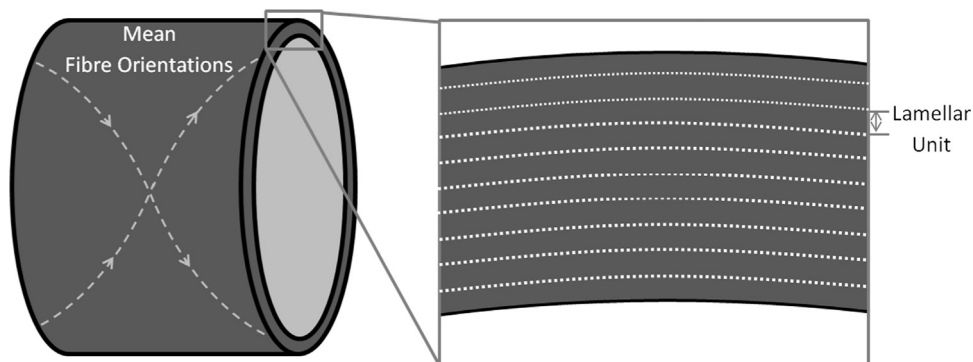


Fig. 2. Idealised representation of the organisation of the aortic media. Families of fibres are oriented predominately into helices around the vessel wall, as shown on the left, with mean orientations closer to circumferential, rather than axial direction. The lamellae are stacked upon one another with interconnecting fibres providing some radial resistance.

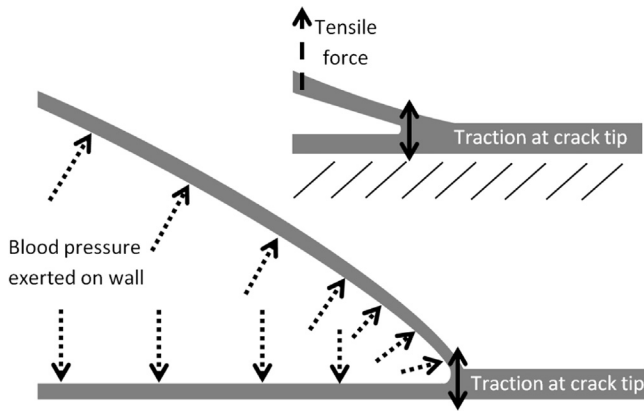


Fig. 3. 2D schematic illustrating the similar tractions at the crack tip for peeling and blood pressure propagation of the dissection.

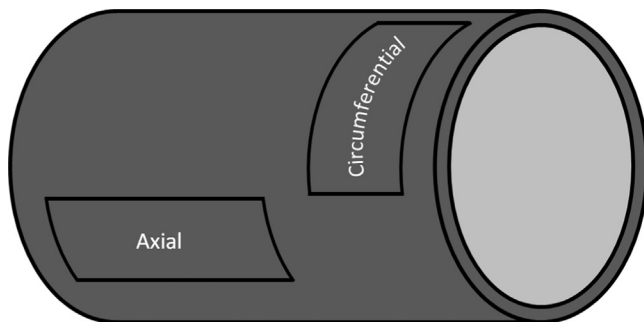


Fig. 4. Schematic showing orientations of sample with respect to the artery wall.

in Sections 4 and 5, the implications of the findings are discussed, and conclusions of the study are presented.

## 2. Methods

### 2.1. Sample preparation

Thoracic aorta from healthy pigs bred for human consumption were collected from a local butcher on the same day as slaughter and transported in a cooled environment to the laboratory. Excess connective tissue was removed and the aortas were cleaned and stored in saline solution. Each aorta was cut into 40 mm by 10 mm strips, oriented either in axial or circumferential (circ) directions (Fig. 4). The adventitia was carefully peeled away and discarded to ensure similar mechanical properties on either side of the tear when peeled. The intima was deemed to be too thin to have a significant influence on the mechanical response, and was therefore not removed. Finally a tear was initiated by making a small incision through the centre of the media.

Collagenase, elastase and glutaraldehyde treatments were performed according to the protocols described previously (Noble et al., 2016), and as further summarised in Table 1. Control and treated tissue was tested within 48 hours of the slaughter of the animal, (this period included both retrieval of tissue from the supplier and incubation according to the described protocols). After treatment all samples were washed thoroughly in saline solution and stored in saline solution plus antibiotic and anti-fungals at room temperature prior to testing.

### 2.2. Test protocol

Samples were prepared for peel testing by carefully pulling apart the flaps either side of the incision to leave 10 mm of tissue tongues for the tensile machine grips to hold. To measure sample geometry, samples were photographed using a Fujifilm Finepix Z90 digital camera with a ruler adjacent for scale (Fig. 5). Sample width and peeled length were then estimated using ImageJ software<sup>1</sup>. Mean sample geometries are summarised in Table 2a and b. After photographing, samples were placed back in PBS solution for 5 s to rehydrate before mounting in the tensile test machine grips. Peel testing was performed at room temperature on a Tinius Olsen 5 kN tensile

Table 1

Enzyme, glutaraldehyde and control treatment concentrations and durations. N (axial) and N(circ) are the number of treated samples in the axial and circumferential direction respectively.

Treatment	Concentration	Temp.	Duration	N(axial)	N(circ)
Control	–	37 °C	20 h	16	16
Collagenase (Roche)	0.05 U/ml	37 °C	20 h	14	17
Elastase (Sigma Aldrich)	0.2 U/ml	37 °C	20 h	14	16
Glutaraldehyde	0.1%	4 °C	20 h	14	13

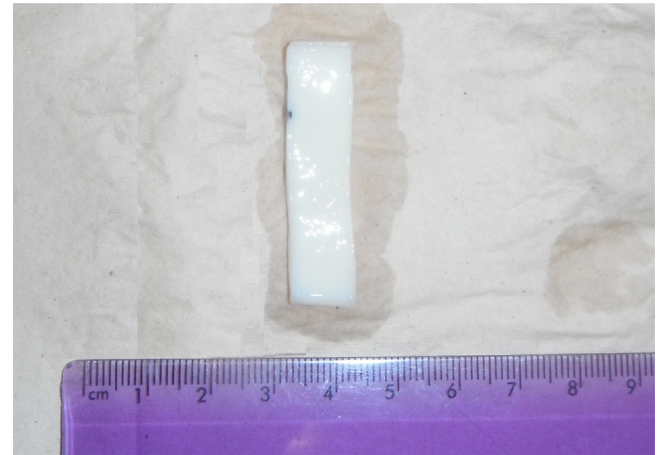


Fig. 5. Sample before peeling. The initial tear began at the top of the specimen and extended to the black marker.

machine with a 10 N Tinius Olsen load cell. The samples were mounted such that the machine grips were as close to the start of the tear as possible. Grip surfaces were serrated to prevent slippage. Gradual loading was applied until 0.05 N force was registered, to place the sample in tension just prior to testing. The machine head was then displaced at 1 mm/s to peel the sample apart. A study by van Baardwijk and Roach (1987) suggests dissection speeds may vary significantly under pulsatile blood pressure loads. The peeling speed used here, which lies near the middle of the range identified in van Baardwijk and Roach (1987), was thus selected to approximate the physiological loading rates experienced by the tissue during an intervention, whilst ensuring controlled peeling was maintained. Additionally, the time during which samples were out of saline solution was minimised, to ensure they remained hydrated. If the sample broke before the two sides had completely peeled, it was discarded. The experimental configuration is illustrated in Fig. 6.

### 2.3. Critical energy release rate

As in Sommer et al. (2008), we utilise the critical energy release rate ( $G_c$ ) to quantify the peeling response. This is found in either the axial or circumferential direction as follows:

$$G_c = (W_{ext} - W_{elastic})/L \quad (1)$$

where  $W_{ext}$  and  $W_{elastic}$  are the externally applied work and stored energy per unit width, and  $L$  is the length of tissue to be dissected, shown in Fig. 6.  $W_{ext}$  is computed using:

$$W_{ext} = 2Fl \quad (2)$$

where  $F$  is the mean peeling force (per unit width), and  $l$  is the length of the tissue in the stretched state, immediately prior to breaking. Both are illustrated in Fig. 7 (see Fig. 6 for additional explanation of  $l$ ). Eq. (2) can be understood as the tensile machine grip displacement ( $2l$ ) multiplied by the mean peeling force. Equivalently, this can be approximated by twice the area under the steady state region of the curve in Fig. 7. Finally  $W_{elastic}$  is estimated as the mean force per width times the tissue change in length, i.e.:

$$W_{elastic} = F(l-L) \quad (3)$$

wherein linearity of the constitutive response is assumed - see discussion in Sommer et al. (2008).

### 2.4. Multiphoton microscopy

To visualise the effect of enzymatic digestion on collagen and elastin fibres, two photon and second harmonic generation microscopy (TPM and SHG) was performed on

<sup>1</sup> <http://imagej.nih.gov/ij/>

a series of samples created using the same protocols as for the test specimens. It was conducted on a Zeiss Upright LSM510 Meta Confocal Microscope with a class 4 tunable Ti-Sapphire two-photon laser. TPM was conducted at 800 nm to visualise elastin fibres and SHG at 950 nm for collagen. Samples were imaged from the intimal side on the axial-circumferential plane at a depth of 19.5 μm from the surface.

### 3. Results

#### 3.1. Controlled peel testing

Hereafter, superscripts “a” and “c” are used to denote results for axial and circumferential samples, respectively. A common pattern of behaviour can be seen across all samples with a sharp increase to a well defined, but uneven, plateau region, followed by a sudden drop off, as the sample fully separates. This can be seen in Fig. 8.

The mean force values from the plateau regions of each curve were computed and then averaged to find  $F^a$  and  $F^c$ . These are shown in Table 3. Critical energy release rates,  $G_c^a$  and  $G_c^c$ , are shown in Table 3. Further observations of behaviour for each treatment type are presented below:

**Control.** No significant difference ( $p=0.081$ ) was found between  $G_c^a$  and  $G_c^c$  for the control samples (Table 3). The force plateau regions for most samples (though for axial samples in particular) were quite noisy, and the spread of values between samples was relatively high. Standard deviations for  $F^a$  and  $F^c$  were therefore similarly high (with the standard deviation of  $F^a$  largest). Correspondingly, though  $G_c^a$  was larger than  $G_c^c$ , the difference was not significant.

**Collagenase.**  $G_c^a$  was significantly greater ( $p=0.014$ ) than  $G_c^c$ . Comparing to the control samples,  $G_c^a$  and  $G_c^c$  were both significantly

lower (Table 3). There was little difference in curve profiles or spread between circumferential and axial directions, as reflected in the standard deviations of  $F^a$  and  $F^c$ .

**Elastase.** No significant difference was observed between  $G_c^a$  and  $G_c^c$  ( $p=0.068$ ) and both were similar to the control samples (Table 3). The pattern of higher noise in axial results is also observed here, again also seen in the standard deviation of  $F^a$  being far greater than that of  $F^c$ .

**Glutaraldehyde.**  $G_c^a$  and  $G_c^c$  were also similar, with  $G_c^c$  slightly, but not significantly, higher ( $p=0.838$ ). Comparing with control samples, there was a significant increase in  $G_c^c$ , but no significant difference in  $G_c^a$  (Table 3). Unlike the control and elastase treated samples, the noisiness of the plateau region and spread of data were greater in the circumferential direction. This can also be seen in Table 3, where the standard deviation of  $F^c$  is greater than that of  $F^a$ .

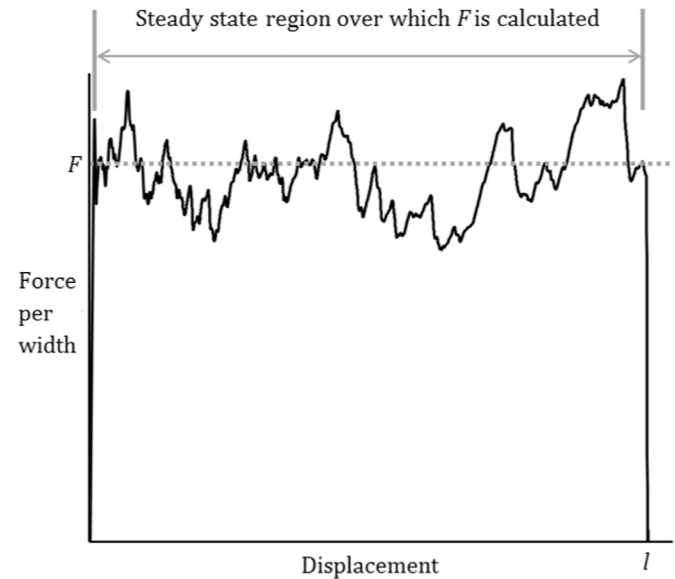


Fig. 7. Representation of the force displacement data from a peel test, and indicating the region over which the mean peeling force  $F$  is calculated. The displacement  $l$  of the loading grips at full separation is also shown.

Table 2  
Mean ± standard deviation of sample dimensions.

	Control	Collagenase	Elastase	Glutaraldehyde
(a) Width of tissue (mm).				
Axial	9.4 ± 1.2	9.3 ± 0.8	9.3 ± 0.7	9.9 ± 1.1
Circumferential	9.4 ± 1.2	9.7 ± 0.6	9.7 ± 0.7	10.1 ± 0.9
(b) Length of tissue to be dissected (mm).				
Axial	31.4 ± 1.4	30.1 ± 2.1	30.9 ± 1.5	30.2 ± 1.9
Circumferential	31.5 ± 2.3	29.3 ± 2.2	30.5 ± 1.4	31.9 ± 3.1

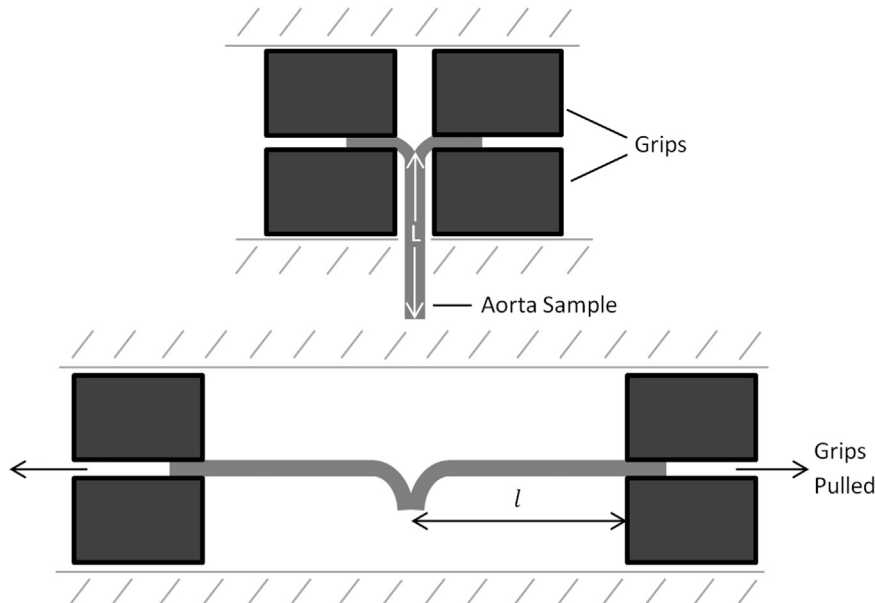


Fig. 6. Schematic of experimental set up before loading and immediately before full separation. The top image shows the free tongues, made by the initial manual tearing, held by grips.  $l$  is the length of tissue to be dissected. In the bottom image,  $l$  is the length of the tissue at full separation.

### 3.2. Microscopy

Multiphoton images of the elastin and collagen in control samples and the samples after partial digestion of the respective proteins are shown in Fig. 9. It can be seen that there is a clear loss of each respective fibre after digestion with both collagenase and

elastase. The remaining collagen fibres appear more wavy and less distinct, with more empty space visible and thinner fibres missing, while there appears to be little remaining structure to the elastin fibres. Finally, it appears glutaraldehyde treatment caused an increase in fibre crosslinks and fibre density for both collagen and elastin.

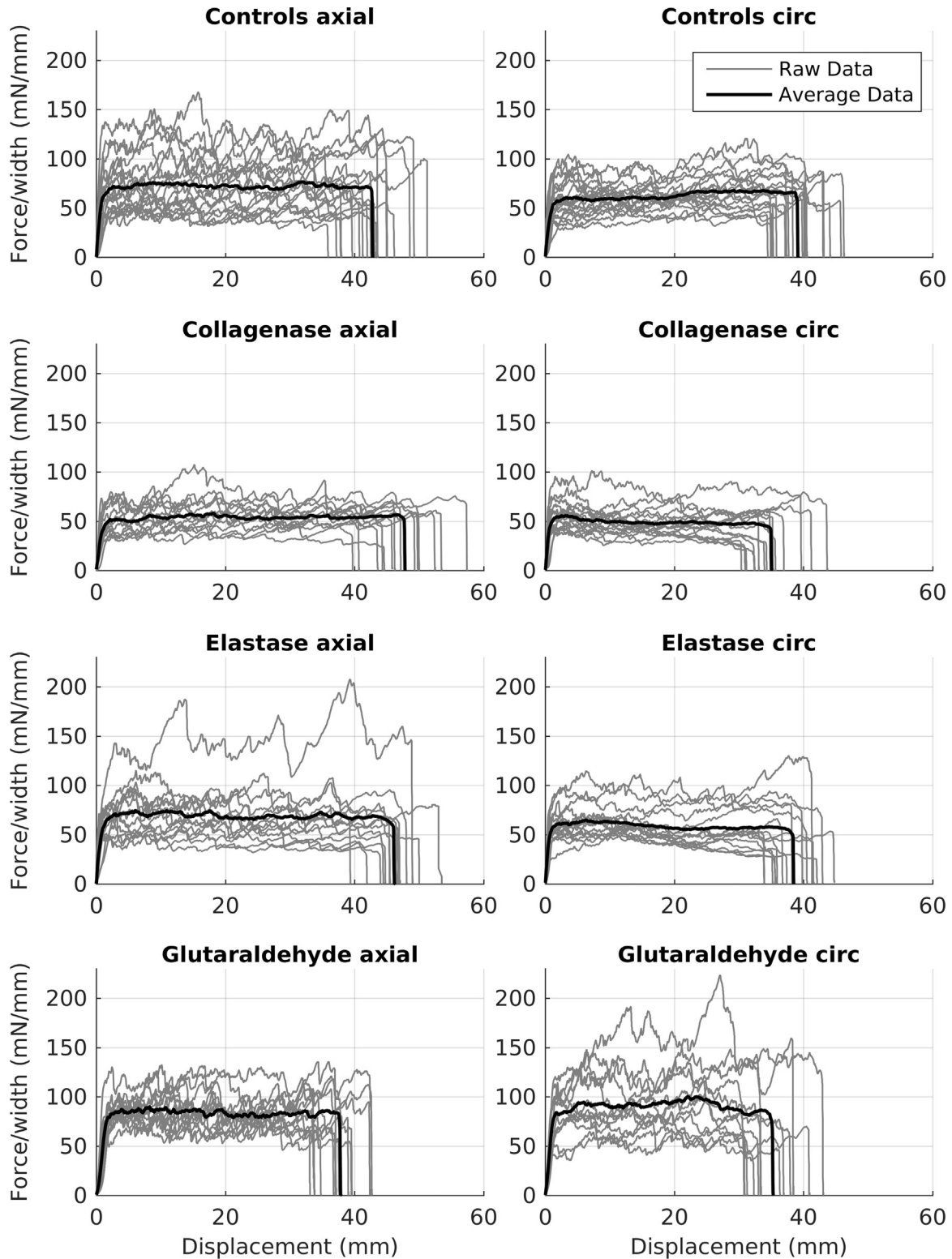


Fig. 8. Force per unit width versus displacement for peel tests in the axial and circumferential directions.

**Table 3**

Average steady state forces per unit width and critical energy release rates  $\pm$  standard deviations, with associated p values compared with control results. Units for  $F$  and  $G_c$  are N/m and J/m<sup>2</sup>, respectively. p values were calculated from  $G_c$  data using Student's unpaired *t*-test.

Value	Control	Collagenase	Elastase	Glutaraldehyde
(a) Axial.				
$F^a$	76.7 $\pm$ 25.9	53.9 $\pm$ 12.2	69.1 $\pm$ 27.0	83.6 $\pm$ 13.7
$G_c^a$	183.3 $\pm$ 64.2	135.8 $\pm$ 31.2	171.8 $\pm$ 71.2	186.3 $\pm$ 33.5
p value	N/A	0.018	0.647	0.876
(b) Circumferential.				
$F^c$	67.4 $\pm$ 11.7	49.3 $\pm$ 11.9	58.8 $\pm$ 17.3	91.2 $\pm$ 28.2
$G_c^c$	151.8 $\pm$ 27.0	108.1 $\pm$ 28.0	132.4 $\pm$ 40.0	190.1 $\pm$ 60.5
p value	N/A	< 0.001	0.118	0.031

#### 4. Discussion

The noisy force profiles yielded by all samples are similar to those described elsewhere for peel testing and other forms of arterial tearing (Sommer et al., 2008; Tong et al., 2011). They most likely stem from the fibrous structure of the arterial wall. Separation of the neighbouring layers, correspondingly, is characterised by progressive breaking of individual fibres, or of larger fibre bundles, so that the overall failure process more closely resembles a series of discrete failure events, rather than a single continuous one. Similar effects have been observed in rubber as so-called stick-slip tearing.

Previous work has highlighted anisotropy in the peeling behaviour of arterial walls (Sommer et al., 2008). The axial direction was shown to exhibit more erratic behaviour, with the plateau region being less flat and with greater variation between samples compared to the circumferential direction. This was also seen for  $F^a$  and  $G_c^a$  in this study: both were higher and had greater standard deviations than did their circumferential counterparts. This is again thought to be related to the fibrous structure of the tissue.

Of the previous studies we identified (Table 4), our values for  $G_c^c$  in control samples (151.8  $\pm$  27 J/m<sup>2</sup>) were closest to those of Carson and Roach (Carson and Roach, 1990), who reported a  $G_c$  of 159  $\pm$  9 J/m<sup>2</sup> (though the orientation of their specimens was not reported). In that study, porcine thoracic aorta was used (as here) however, the tearing was propagated via liquid infusion, rather than peeling. The patterns of deformation, and corresponding modes of failure were therefore different from those in our experiments (see Section 1), and care must be taken in drawing comparisons. Results of other liquid infusion studies, for example, corresponded less well with our values, with the possible exception of lower abdominal aorta results from Roach and Song (1994). Our force and energy measurements were generally much higher than those of previous peel test studies, with the exception of Pasta et al. (Pasta et al., 2012), whose  $F^a$  and  $F^c$  values were significantly higher again. Furthermore, this range of values is not unexpected considering the variability in response of arterial walls subjected to tensile loading in the axial and circumferential directions: average constitutive parameters (fitted to biaxial tensile test data) of control samples from two similar studies were over an order of magnitude different (Gundiah et al., 2013; Zeinali-Davarani et al., 2013). Nevertheless the values for  $F_a$ ,  $F_c$ ,  $G_c^a$  and  $G_c^c$  reported here lie in the range of those found in the literature, providing confidence in their reliability.

##### 4.1. Collagenase

The significant drop in  $G_c^a$  and  $G_c^c$  compared to control samples implies that collagen has a large effect on peeling response. The microscopy results also show a clear loss of collagen fibres and resulting structure. This supports the literature on Ehlers-Danlos syndrome presented in the introduction, in which collagen loss

was noted to correlate with higher rates of dissection. Additionally previous studies reported that collagen lies between lamellae and that toward the centre of this interlamellar space the fibres are randomly orientated (Dingemans et al., 2000).

The difference between  $G_c^a$  and  $G_c^c$  increased in the collagenase treated samples, which is contradictory to results from tensile tests wherein anisotropy decreased with decreasing collagen content (Schriefel et al., 2015). However, the overall spread of  $G_c^a$  and  $G_c^c$  (as measured by the standard deviation) became more similar, implying that treatment reduced the variability between samples. The mechanisms by which collagenase reduces inter-sample variation are not clear, but differences in collagen density and cross-linking likely contribute to the variation between animals and location. Digestion of collagen may correspondingly reduce this variation.

The steady state regions of the force responses are smoother for collagenase samples than for controls (in both directions), which may reflect both reduced concentration of collagen fibres and lower strength of remaining fibres. These findings are similar to those of our previous study on tensile behaviour of treated tissues, where only collagenase treated samples showed a statistically significant drop in fracture stress compared to controls (Noble et al., 2016).

##### 4.2. Elastase

Overall, there was little difference between the control and elastase treated samples, with no statistically significant differences in either  $G_c^a$  or  $G_c^c$ . However, the microscopy images show large loss of elastin and nearly all fibre structure. This suggests elastin plays a lesser role than collagen in the tissues' resistance to controlled peeling.

On the other hand, while affirming a primary organisation into tangentially oriented sheets, Clark and Glagov (1985); Dingemans et al. (2000); O'Connell et al. (2008) noted elastin struts between lamellae and interlamellar elastin fibers that may provide some radial resistance. Moreover, MacLean et al. (MacLean et al., 1999) observed breakages in these small elastin fibres following radial loading of aorta samples, suggesting they would indeed bear some of the load applied in this study. Viewed in this light, then, the present results may rather reflect either very low strength in these small fibres so that the effect of their degradation was not detectable in our experiments, or inadequate permeation of the enzyme to the centre of the samples, where these fibres reside. Whatever the true mechanism, it is clear that the elastase treatment, in contrast to its influence on tensile behaviour, had little effect on the peeling behaviour of the aorta samples.

##### 4.3. Glutaraldehyde

Glutaraldehyde has been previously utilised for cross-linking collagen to increase material stiffness and tensile strength (Damink et al., 1995; Hapach et al., 2015). In this work, glutaraldehyde was the only treatment to show increases in  $G_c^a$  and  $G_c^c$  compared to controls, though only the circumferential increases were significant ( $p < 0.05$ ). In contrast, our previous study found little effect of glutaraldehyde treatment on the tensile elastic and fracture properties of porcine aorta (Noble et al., 2016). However, microscopy images in the axial-circumferential plane showed increased crosslinking and fibre density. Therefore, this implies that partial cross-linking resulting from low concentration glutaraldehyde treatment is more effective in the radial direction than in the axial or circumferential directions.

##### 4.4. Diseased tissue comparison

Few studies have investigated the effect of disease on tissue response under controlled peeling. Difficulties in finding a significant number of participants for relatively rare genetic diseases like Marfan's and Ehlers-Danlos syndrome prevent investigation into the biomechanical effects of these diseases.

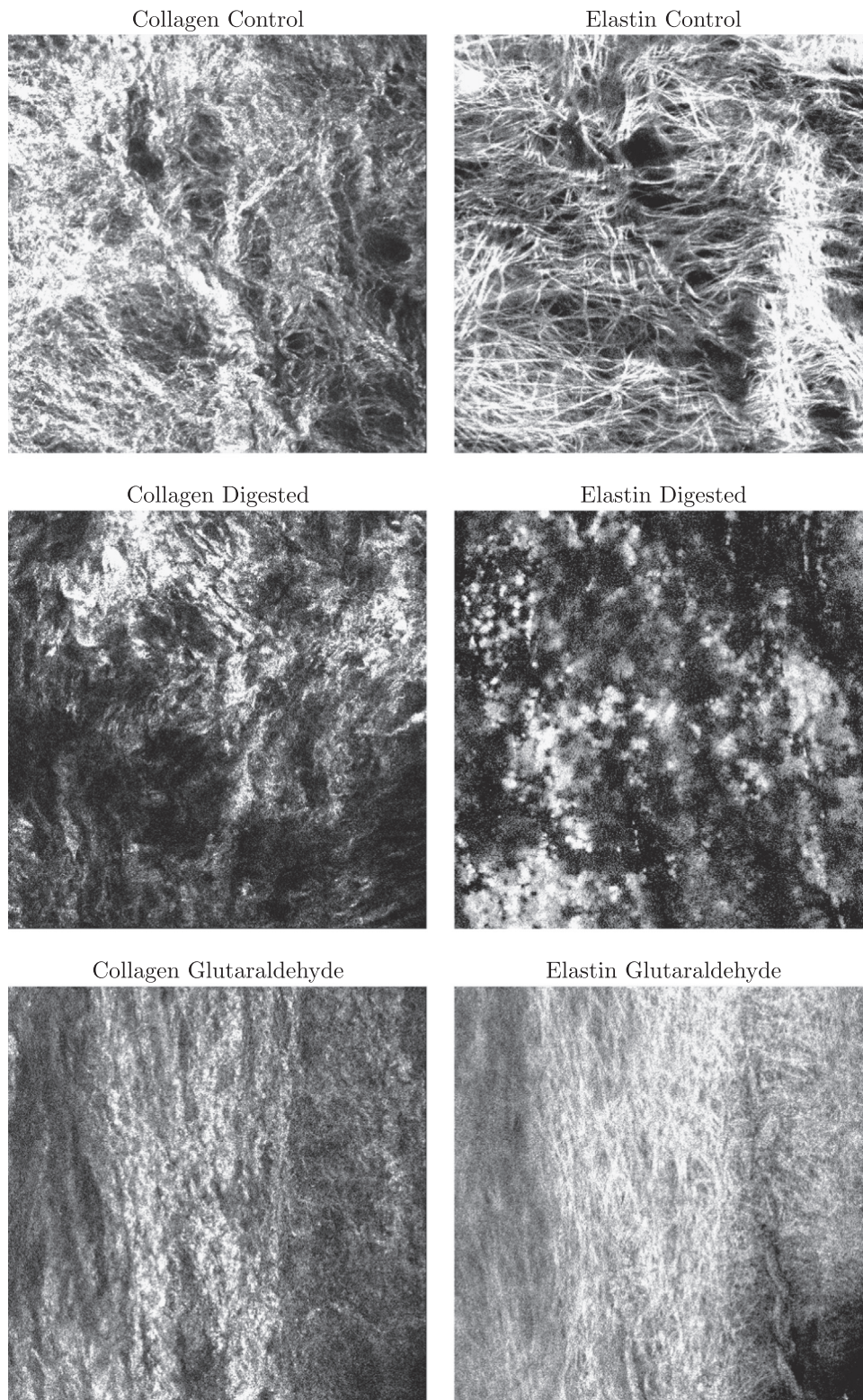


**Fig. 9.** SHG images of collagen and TPM images of elastin (at depth of 19.5  $\mu\text{m}$ ) for controls, samples with either proteins digested by their respective enzyme and each protein following glutaraldehyde treatment. Intimal side of the axial-circumferential plane is presented to demonstrate the protein loss.

However, peel tests have been performed on aneurysm tissue from ascending thoracic aorta and compared to healthy tissue from the same location (Pasta et al., 2012). They found that both  $F^a$  and  $F^c$  for aneurysm tissue were significantly lower than for healthy tissue and that the difference between  $F^a$  and  $F^c$  was decreased in aneurysm tissue, indicating a loss of anisotropy. This behaviour is most like that of the collagenase digested tissue reported here. However, aneurysms

are more strongly associated with elastin loss, which we found to have negligible effect on controlled peel testing of arterial samples.

#### 4.5. Limitations

The direct effects of genetic diseases, such as Ehlers-Danlos and Marfan's syndrome, on arterial wall constituent proteins are

**Table 4**  
Healthy artery peeling forces per width,  $F_a$ ,  $F_c$  (N/m), and critical energy release rates,  $G_c^a$ ,  $G_c^c$  (J/m<sup>2</sup>). P, porcine and H, human. A, aorta; TA, thoracic aorta; ATA, UTA and LTA, ascending, upper and lower thoracic aorta; AA, abdominal aorta; UAA and LAA, upper and lower abdominal aorta; ICA and CCA, internal and common carotid artery; CA, coronary artery. LI, liquid infusion.

Vessel	Method	$F_a$	$F_c$	$G_c^a$	$G_c^c$	Ref.
P-UTA	LI	–	–	159 ± 9	–	Carson and Roach, 1990
H-A	LI	–	–	16.5	–	Tiessen and Roach (1993)
P-ATA	LI	–	–	43.9 ± 21.9	–	Roach and Song (1994)
P-UTA	LI	–	–	28.4 ± 11.9	–	Roach and Song (1994)
P-LTA	LI	–	–	29 ± 12.1	–	Roach and Song (1994)
P-UAA	LI	–	–	18.8 ± 8.9	–	Roach and Song (1994)
P-LAA	LI	–	–	113.4 ± 40.5	–	Roach and Song (1994)
H-AA	Peeling	34.8 ± 15.5	22.9 ± 2.9	76 ± 27	51 ± 6	Sommer et al. (2008)
H-ICA	Peeling	26.9 ± 7.1	–	60 ± 16	–	Tong et al. (2011)
H-CCA	Peeling	33.7 ± 10.9	21.5 ± 4.2	75 ± 24	48 ± 10	Tong et al. (2011)
H-ATA	Peeling	149.0 ± 7.6	126.0 ± 6.6	–	–	Pasta et al. (2012)
H-CA	Peeling	–	–	10.3 ± 5	–	Wang et al. (2014)
P-TA	Peeling	76.7 ± 25.9	67.4 ± 11.7	183.3 ± 64.2	151.8 ± 27.0	Present

relatively simple to understand and emulate. However in an individual with such diseases, compensatory processes in the body will alter the mechanical response of the wall beyond the effect of simple enzyme digestion, thus requiring insight into the change in arterial wall structure by these processes. Additionally, for more complex diseases such as aneurysms, simple enzymatic digestion provides only an approximation of the various chemical, physical and cellular processes taking place within the arterial wall. However, the treatments described here appear to approximate the changes in dissection properties reported to accompany Ehlers-Danlos and Marfan's syndrome and provide similarities in behaviour for more complex processes such as aneurysms. Furthermore, more accurate emulation of dissection properties may also be produced using a combination of any or all of these treatments.

While smooth muscle cells do bridge the lamellae we assumed their effect on the tissue response to controlled peeling was small, compared with those of collagen and elastin. Nevertheless it has been shown that smooth muscle cells do play a role in arterial dissection *in vivo* (Luo et al., 2009; Guo et al., 2007). A dedicated investigation into the effect of removing smooth muscle cell contribution (for example by means described in Marano et al. (1999)) in controlled peeling conditions would help to clarify their role.

Previous studies performed peel tests within a saline bath, whilst in this study testing was conducted at room temperature and in open air. Peel tests took around 90 s, and specimens were exposed to air for around four minutes on average. Utilising a saline bath at 37 °C may yield results with more physiological relevance, however since all tests were performed under the same conditions the comparisons made here are still valid.

The loading rate applied to the samples is greater than that applied in previous studies. Tong et al. investigated the effect of peeling rate on the tissue response (Tong et al., 2014). They found approximately 30% difference in  $F$  between samples tested at 1 mm/min and 1 m/s, a significantly smaller difference than between our findings and results from other studies presented in Table 4. This suggests speed alone does account for the discrepancy and variation between samples, as described in the opening of the Discussion, may play a greater role.

Mechanical tests (of any kind) do not allow changes in the arterial wall microstructure to be observed directly, even if some overall changes may be inferred from their results. Example images acquired with multiphoton microscopy, and in the axial-circumferential plane, were presented here, to enable qualitative assessment of structural changes. But, more detailed and systematic visual analysis using these modalities (Tsamis et al., 2013), or perhaps histology (Tong et al., 2011) or electron microscopy (O'Connell et al., 2008) would enable microstructural changes to be assessed conclusively, and may present

a link between elastin/collagen radial fibre bridging and gross mechanical properties.

Finally, in this work the samples were tested as flat rectangular pieces, while *in vivo*, the vessel is tubular and held in a pre-stressed state that is partially release by cutting the vessel open to lay it flat. The effect of this difference on the dissection propagation and on measured values such as the  $F$  and  $G_c$  are unknown, as previous work, either peel testing or liquid infusion testing, also involved flat samples. An investigation into the dissection behaviour of the artery wall in its *in vivo* configuration would help to clarify the effect of flattening the tissue in this way.

## 5. Conclusions

Applying collagenase solution to porcine thoracic aorta made the tissue less resistant to peeling in both axial and circumferential directions. However, anisotropy in the critical energy release rate was increased compared to control samples. Elastase treatment had a negligible effect on the tissue response to controlled peel testing. From these it may be inferred that collagen plays a more important role in resisting this loading mechanism. Glutaraldehyde treatment increased resistance to peeling in both directions, but more so in the circumferential direction. Anisotropy in the response was correspondingly reduced. Thus, cross-linking accompanying this treatment appears to impart greater strength in the circumferential direction.

Of the treatments considered, the effects of collagenase most closely resembled those of aneurysm formation. This is despite elastin loss being more commonly associated with this condition. Regardless of the possible difference in underlying mechanisms, collagenase treatment appears to be a viable means of altering the peeling response of aortic tissues to emulate the effects of this disease. Combined with those of our previous work on the effects on tensile properties (Noble et al., 2016), these findings suggest that all of the described treatments are useful in creating physical models of diseased tissue.

## Conflict of interest

The authors have no conflict of interest.

## Acknowledgements

This work was supported by the Engineering and Physical Sciences Research Council (Doctoral Training Grant) and the European Commission Framework Programme 7, Understanding Interactions

of Human Tissue with Medical Devices (UNITISS, FP7-PEOPLE-2011-IAPP/286174).

Imaging work was performed at the Kroto Research Institute Confocal Imaging Facility, using the LSM510 Meta upright confocal microscope.

## References

- Adams Jr., H.P., Aschenbrenner, C.A., Kassell, N.F., Ansbacher, L., Cornell, S.H., 1982. Intracranial hemorrhage produced by spontaneous dissecting intracranial aneurysm. *Arch. Neurol.* 39, 773–776.
- Anagnostopoulos, C.E., Prabhakar, M.J., Kittle, C.F., 1972. Aortic dissections and dissecting aneurysms. *Am. J. Cardiol.* 30, 263–273. [http://dx.doi.org/10.1016/0002-9149\(72\)90070-7](http://dx.doi.org/10.1016/0002-9149(72)90070-7).
- Bonnet, J., Aumailley, M., Thomas, D., Grosogeat, Y., Broustet, J.P., Bricaud, H., 1986. Spontaneous coronary artery dissection: case report and evidence for a defect in collagen metabolism. *Eur. Heart J.* 7, 904–909.
- Carson, W., Roach, M.R., 1990. The strength of the aortic media and its role in the propagation of aortic dissection. *J. Biomech.* 3, 579–588. [http://dx.doi.org/10.1016/0021-9290\(90\)90050-D](http://dx.doi.org/10.1016/0021-9290(90)90050-D).
- Clark, J.M., Glagov, S., 1985. Transmural organization of the arterial media. the lamellar unit revisited. *Arteriosclerosis* 5, 19–34. <http://dx.doi.org/10.1161/01.ATV.5.1.19>.
- Dadgar, L., Marois, Y., Deng, X., Guidoin, R., 1997. Arterial wall mechanical characteristics after treatment in collagenase: an in vitro aneurysm model. *Clin. Investig. Med.* 20, 25–34.
- Damink, L.H.H.O., Dijkstra, P.J., Van Luyn, M.J.A., Van Wachem, P.B., Nieuwenhuis, P., Feijen, J., 1995. Glutaraldehyde as a crosslinking agent for collagen-based biomaterials. *J. Mater. Sci.: Mater. Med.* 6, 460–472. <http://dx.doi.org/10.1007/BF00123371>.
- Dingemans, K.P., Teeling, P., Legendijk, J.H., Becker, A.E., 2000. Extracellular matrix of the human aortic media: an ultrastructural histochemical and immunohistochemical study of the adult aortic media. *Anat. Rec.* 258, 1–14. [http://dx.doi.org/10.1002/\(SICI\)1097-0185\(20000101\)258:1;1::AID-AR1;3.0.CO;2-7](http://dx.doi.org/10.1002/(SICI)1097-0185(20000101)258:1;1::AID-AR1;3.0.CO;2-7).
- de Figueiredo Borges, L., Jaldin, R.G., Dias, R.R., Stolf, N.A.G., Michel, J.B., Gutierrez, P. S., 2008. Collagen is reduced and disrupted in human aneurysms and dissections of ascending aorta. *Hum. Pathol.* 39, 437–443. <http://dx.doi.org/10.1016/j.humpath.2007.08.003>.
- Goldfinger, J.Z., Halperin, J.L., Marin, M.L., Stewart, A.S., Eagle, K.A., Fuster, V., 2014. Thoracic aortic aneurysm and dissection. *J. Am. Coll. Cardiol.* 64, 1725–1739. <http://dx.doi.org/10.1016/j.jacc.2014.08.025>.
- Gundiah, N., Babu, A.R., Pruitt, L.A., 2013. Effects of elastase and collagenase on the nonlinearity and anisotropy of porcine aorta. *Physiol. Meas.* 34, 1657–1673. <http://dx.doi.org/10.1088/0967-3334/34/12/1657>.
- Guo, D.C., Pannu, H., Tran-Fadulu, V., Papke, C.L., Yu, R.K., Avidan, N., Bourgeois, S., Estrera, A.L., Safi, H.J., Sparks, E., Amor, D., Ades, L., McConnell, V., Willoughby, C.E., Abuelo, D., Willing, M., Lewis, R.a., Kim, D.H., Scherer, S., Tung, P.P., Ahn, C., Buija, L.M., Raman, C.S., Shete, S.S., Milewicz, D.M., 2007. Mutations in smooth muscle alpha-actin (ACTA2) lead to thoracic aortic aneurysms and dissections. *Nat. Genet.* 39, 1488–1493. <http://dx.doi.org/10.1038/ng.2007.6>.
- Hapach, L.a., Vanderburgh, J.a., Miller, J.P., Reinhart-King, C.a., 2015. Manipulation of in vitro collagen matrix architecture for scaffolds of improved physiological relevance. *Phys. Biol.* 12, 061002. <http://dx.doi.org/10.1088/1478-3975/12/6/061002>.
- He, C.M., Roach, M.R., 1994. The composition and mechanical properties of abdominal aortic aneurysms. *J. Vasc. Surg.* 20, 6–13. [http://dx.doi.org/10.1016/0741-5214\(94\)90169-4](http://dx.doi.org/10.1016/0741-5214(94)90169-4).
- Hirst, A.E., Johns, V.J., 1962. Experimental dissection of media of aorta by pressure: its relation to spontaneous dissecting aneurysm. *Circ. Res.* 10, 897–903.
- Kochová, P., Kuncová, J., Svíglerová, J., Cimrman, R., Miklíková, M., Liška, V., Tonar, Z., 2012. The contribution of vascular smooth muscle, elastin and collagen on the passive mechanics of porcine carotid arteries. *Physiol. Meas.* 33, 1335–1351. <http://dx.doi.org/10.1088/0967-3334/33/8/1335>.
- Luo, F., Zhou, X.L., Li, J.J., Hui, R.T., 2009. Inflammatory response is associated with aortic dissection. *Ageing Res. Rev.* 8, 31–35. <http://dx.doi.org/10.1016/j.arr.2008.08.001>.
- MacLean, N.F., Dudek, N.L., Roach, M.R., 1999. The role of radial elastic properties in the development of aortic dissections. *J. Vasc. Surg.* 29, 703–710. [http://dx.doi.org/10.1016/S0741-5214\(99\)70317-4](http://dx.doi.org/10.1016/S0741-5214(99)70317-4).
- Mamas, M.A., Alonso, A., Neyses, L., 2008. Extensive catheter-induced aortic dissection. *Can. J. Cardiol.* 24, 9–10.
- Marano, G., Grigioni, M., Palazzesi, S., Ferrari, A.U., 1999. Endothelin and mechanical properties of the carotid artery in Wistar-Kyoto and spontaneously hypertensive rats. *Cardiovasc. Res.* 41, 701–707.
- Milewicz, D.M., Dietz, H., Miller, C., 2005. Treatment of aortic disease in patients with marfan syndrome. *Circulation* 111, e150–e157. <http://dx.doi.org/10.1161/01.CIR.0000155243.70456.F4>.
- Noble, C., Smulders, N., Green, N.H., Lewis, R., Carré, M.J., Franklin, S.E., MacNeil, S., Taylor, Z.A., 2016. Creating a model of diseased artery damage and failure from healthy porcine aorta. *J. Mech. Behav. Biomed. Mater.* 60, 378–393. <http://dx.doi.org/10.1016/j.jmbmm.2016.02.018>.
- O'Connell, M.K., Murthy, S., Phan, S., Xu, C., Buchanan, J., Spilker, R., Dalman, R.L., Zarins, C.K., Denk, W., Taylor, C.A., 2008. The three-dimensional micro- and nanostructure of the aortic medial lamellar unit measured using 3D confocal and electron microscopy imaging. *Matrix Biol.* 27, 171–181. <http://dx.doi.org/10.1016/j.matbio.2007.10.008>.
- Pasta, S., Philippini, J.A., Gleason, T.G., Vorp, D.A., 2012. Effect of aneurysm on the mechanical dissection properties of the human ascending thoracic aorta. *J. Thorac. Cardiovasc. Surg.* 143, 460–467. <http://dx.doi.org/10.1016/j.jtcvs.2011.07.058>.
- Roach, M.R., Song, S.H., 1994. Variations in strength of the porcine aorta as a function of location. *Clin. Investig. Med.* 17, 308–318.
- Schrieff, A., Zeindlinger, G., Pierce, D.M., Regitnig, P., Holzapfel, G.A., 2012. Determination of the layer-specific distributed collagen fibre orientations in human thoracic and abdominal aortas and common iliac arteries. *J. R. Soc. Interface* 9, 1275–1286. <http://dx.doi.org/10.1098/rsif.2011.0727>.
- Schrieff, A.J., Schmidt, T., Balzani, D., Sommer, G., Holzapfel, G.A., 2015. Selective enzymatic removal of elastin and collagen from human abdominal aortas: uniaxial mechanical response and constitutive modeling. *Acta Biomater.* 17, 125–136. <http://dx.doi.org/10.1016/j.actbio.2015.01.003>.
- Sommer, G., Gasser, T.C., Regitnig, P., Auer, M., Holzapfel, G.A., 2008. Dissection properties of the human aortic media: an experimental study. *J. Biomech. Eng.* 130, 021007. <http://dx.doi.org/10.1115/1.2898733>.
- Sommer, G., Sherifova, S., Oberwalder, P.J., Dapunt, O.E., Ursomanno, P.A., DeAnda, A., Griffith, B.E., Holzapfel, G.A., 2016. Mechanical strength of aneurysmatic and dissected human thoracic aortas at different shear loading modes. *J. Biomech.* . <http://dx.doi.org/10.1016/j.jbiomech.2016.02.042>
- Srivastava, A., Bradley, M., Kelly, M., 2008. Bilateral carotid artery dissection after high impact road traffic accident. *J. Radiol. Case Rep.* 2, 23–28. <http://dx.doi.org/10.3941/jrcr.v2i5.37>.
- Tiessen, I.M., Roach, M.R., 1993. Factors in the initiation and propagation of aortic dissections in human autopsy aortas. *J. Biomech. Eng.* 115, 123–125.
- Tong, J., Sommer, G., Regitnig, P., Holzapfel, G.A., 2011. Dissection properties and mechanical strength of tissue components in human carotid bifurcations. *Ann. Biomed. Eng.* 39, 1703–1719. <http://dx.doi.org/10.1007/s10439-011-0264-y>.
- Tong, J., Cohnert, T., Regitnig, P., Kohlbacher, J., Birner-Gruenberger, R., Schrieff, a.j., Sommer, G., Holzapfel, G.A., 2014. Variations of dissection properties and mass fractions with thrombus age in human abdominal aortic aneurysms. *J. Biomech.* 47, 14–23. <http://dx.doi.org/10.1016/j.jbiomech.2013.10.027>.
- Tsamis, A., Philippini, J.A., Koch, R.G., Pasta, S., D'Amore, A., Watkins, S.C., Wagner, W.R., Gleason, T.G., Vorp, D.A., 2013. Fiber micro-architecture in the longitudinal-radial and circumferential-radial planes of ascending thoracic aortic aneurysm media. *J. Biomech.* 46, 2787–2794. <http://dx.doi.org/10.1016/j.jbiomech.2013.09.003>.
- Ulbricht, D., Diederich, N.J., Hermanns-Lê, T., Metz, R.J., Macian, F., Piérard, G.E., 2004. Cervical artery dissection: an atypical presentation with Ehlers-danlos-like collagen pathology? *Neurology* 63, 1708–1710. <http://dx.doi.org/10.1212/01.WNL.0000142970.09454.30>.
- van Baardwijk, C., Roach, M.R., 1987. Factors in the propagation of aortic dissections in canine thoracic aortas. *J. Biomech.* 20, 67–73. [http://dx.doi.org/10.1016/0021-9290\(87\)90268-5](http://dx.doi.org/10.1016/0021-9290(87)90268-5).
- Wang, Y., Johnson, J.A., Spinale, F.G., Sutton, M.A., Lessner, S.M., 2014. Quantitative measurement of dissection resistance in intimal and medial layers of human coronary arteries. *Exp. Mech.* 54, 677–683. <http://dx.doi.org/10.1007/s11340-013-9836-0>.
- Weisbecker, H., Viertler, C., Pierce, D.M., Holzapfel, G.A., 2013. The role of elastin and collagen in the softening behavior of the human thoracic aortic media. *J. Biomech.* 46, 1859–1865. <http://dx.doi.org/10.1016/j.jbiomech.2013.04.025>.
- Wityk, R.J., Zanferrari, C., Oppenheimer, S., 2002. Neurovascular complications of marfan syndrome. *Stroke* 33, 680–684. <http://dx.doi.org/10.1161/hs0302.1038.16>.
- Wolinsky, H., Glagov, S., 1967. A lamellar unit of aortic medial structure and function in mammals. *Circ. Res.* 20, 99–111. <http://dx.doi.org/10.1161/01.RES.20.1.99>.
- Zeinali-Davarani, S., Chow, M.J., Turcotte, R., Zhang, Y., 2013. Characterization of biaxial mechanical behavior of porcine aorta under gradual elastin degradation. *Ann. Biomed. Eng.* 41, 1528–1538. <http://dx.doi.org/10.1007/s10439-012-0733-y>.